ELSEVIER

Biochimica et Biophysica Acta 1512 (2001) 64–76

BIOCHIMICA ET BIOPHYSICA ACTA
BBA

www.bba-direct.com

Analysis of antimicrobial peptide interactions with hybrid bilayer membrane systems using surface plasmon resonance

Henriette Mozsolits [a], Hans-Jürgen Wirth [a], Jerome Werkmeister [b], Marie-Isabel Aguilar [a,*]

[a] *Department of Biochemistry and Molecular Biology, Monash University, P.O. Box 13D, Clayton, Vic. 3800, Australia*
[b] *CSIRO, Division of Molecular Science, Parkville, Vic. 3052, Australia*

Received 22 November 2000; received in revised form 22 February 2001; accepted 28 February 2001

Abstract

The lipid binding behaviour of the antimicrobial peptides magainin 1, melittin and the C-terminally truncated analogue of melittin (21Q) was studied with a hybrid bilayer membrane system using surface plasmon resonance. In particular, the hydrophobic association chip was used which is composed of long chain alkanethiol molecules upon which liposomes adsorb spontaneously to create a hybrid bilayer membrane surface. Multiple sets of sensorgrams with different peptide concentrations were generated. Linearisation analysis and curve fitting using numerical integration analysis were performed to derive estimates for the association (k_a) and dissociation (k_d) rate constants. The results demonstrated that magainin 1 preferentially interacted with negatively charged dimyristoyl-L-α-phosphatidyl-DL-glycerol (DMPG), while melittin interacted with both zwitterionic dimyristoyl-L-α-phosphatidylcholine and anionic DMPG. In contrast, the C-terminally truncated melittin analogue, 21Q, exhibited lower binding affinity for both lipids, showing that the positively charged C-terminus of melittin greatly influences its membrane binding properties. Furthermore the results also demonstrated that these antimicrobial peptides bind to the lipids initially via electrostatic interactions which then enhances the subsequent hydrophobic binding. The biosensor results were correlated with the conformation of the peptides determined by circular dichroism analysis, which indicated that high α-helicity was associated with high binding affinity. Overall, the results demonstrated that biosensor technology provides a new experimental approach to the study of peptide-membrane interactions through the rapid determination of the binding affinity of bioactive peptides for phospholipids.

Keywords: Peptide-lipid interaction; Surface plasmon resonance; Hybrid bilayer membrane; Circular dichroism; Membrane affinity; Antimicrobial peptide

1. Introduction

Interactions between bioactive peptides and cell membranes play a key role in a number of cellular processes, including the insertion and folding of membrane proteins, the formation and structure of ion channels, the interaction of hormones with membrane receptors and the action of antimicrobial and cytotoxic peptides. The common structural feature of all these classes of molecules is the adoption of a stable secondary structure upon binding to the membrane surface. In the case of antimicrobial peptides,

* Corresponding author. Fax: +61-3-9905-5882;
E-mail: mibel.aguilar@med.monash.edu.au

0005-2736/01/$ – see front matter
PII: S0005-2736(01)00303-0

such as magainin [1,2], melittin [2,3] and cecropin [4], which act by perturbing the barrier function of the cell membrane [5,6], the induction of cationic, amphipathic α-helical structure is thought to play an essential role in their biological activity.

There have been several studies largely using model membrane systems [7,8] aimed at characterising the mechanism of membrane permeabilisation by antimicrobial peptides. A number of physicochemical properties, such as peptide charge, hydrophobicity, amphipathicity and the degree of secondary structure angle subtended by the polar face, have all been shown to play a role in the cell-lytic properties of these peptides. However, since selective binding to different phospholipids is central to the design of non-haemolytic antimicrobial peptides, the affinity of the peptide for the membrane surface is also a critical factor in the cell-lytic process, but is not commonly measured and reported. This is largely due to the difficulty in generating these data, since membrane binding assays generally require a physical separation step, such as dialysis or centrifugation which can be tedious for large numbers of samples [9,10]. Alternatively, peptide partitioning can be directly measured by changes in fluorescence quenching or enhancement of tryptophan fluorescence which relies on the presence of a fluoroprobe. If an intrinsic fluoroprobe is not present, the probe must be incorporated by covalent modification of the peptide and/or the lipid [11,12].

We have developed a new and sensitive method based on surface plasmon resonance (SPR), which allows the real-time measurement of peptide binding to phospholipid membranes. In the present study, the lipid binding characteristics, in terms of their relative affinity, of two antimicrobial peptides magainin 1, melittin and a truncated analogue of melittin (21Q) with a hybrid bilayer membrane (HBM) system of different surface charge have been studied. Small unilamellar vesicles were adsorbed onto the surface of a hydrophobic association (HPA) chip to form a hybrid lipid bilayer that is similar to the surface of a cellular membrane. The binding of antimicrobial peptides to this surface and the resulting data allow the analysis of peptide-lipid interactions and provide a basis to calculate rate constants associated with the interactions. The results demonstrate that biosensor technology has the ability to provide insight into the relationship between the structure of a peptide and its biological activity and membrane selectivity through the lipid binding affinity data.

2. Materials and methods

2.1. Chemicals and reagents

N-Octyl β-D-glucopyranoside, dimyristoyl-L-α-phosphatidylcholine (DMPC), dimyristoyl-L-α-phosphatidyl-DL-glycerol (DMPG) and the negative control, bovine serum albumin (BSA), were purchased from Sigma (St Louis, MO, USA). Cytolytic peptides, melittin and magainin 1 were purchased from Auspep (Parkville, Vic., Australia). The truncated analogue of melittin (21Q) was synthesised by solid phase peptide synthesis, purified by reversed phase high performance liquid chromatography (RP-HPLC) and characterised by amino acid analysis and matrix-assisted laser desorption mass spectrometry as previously described [13]. Water was quartz-distilled and deionised in a Milli-Q system (Millipore, Bedford, MA, USA).

2.2. Biosensor study

Biosensor experiments were carried out with a BIAcore X analytical system (Biacore, Uppsala, Sweden) using an HPA sensor chip (Biacore). The HPA sensor chip is composed of long chain alkanethiol molecules covalently linked to the gold surface to form a hydrophobic monolayer. The running buffer used for all experiments was phosphate buffer (0.02 M NaH_2PO_4/Na_2HPO_4, pH 6.8). The washing solution was *N*-octyl β-D-glucopyranoside (40 mM). The regeneration solution was sodium hydroxide (10 mM). All solutions were freshly prepared, degassed and filtered through a 0.22 μm filter. The operating temperature was 25°C. The sequence and molecular mass of all peptides used are listed in Table 1.

2.2.1. Liposome preparation

Small unilamellar vesicles (SUV; 50 nm) of DMPC or DMPG were prepared in 0.02 M phosphate buffer by sonication. Briefly, dry DMPC was dissolved in ethanol-free chloroform or in the case of DMPG the dry lipid was dissolved in a $CHCl_3$/MeOH mixture

(2:1, v/v). In both cases the solvent was evaporated under a stream of nitrogen, and the lipids were held under vacuum overnight. The lipids were then resuspended in 0.02 M phosphate buffer, via vortex mixing. The resultant lipid dispersion (a concentration of 0.5 mM with respect to phospholipid) was then sonicated in a bath type sonicator until clear.

2.2.2. Formation of hybrid bilayer membranes (HBM)

After cleaning as outlined in the instrument manual, the BIAcore X instrument was left running overnight using Milli-Q water as eluent to thoroughly wash all liquid handling parts of the instrument. The HPS sensor chip was then installed and the alkanethiol surface was cleaned by an injection of the non-ionic detergent 40 mM octyl glucoside (25 μl), at a flow rate of 5 μl/min. SUV (30 μl, 0.5 mM) were then immediately applied to the chip surface at a low flow rate (2 μl/min). To remove any multilamellar structures from the lipid surface, sodium hydroxide (30 μl, 10 mM) was injected at a flow rate of 50 μl/min which resulted in a stable baseline corresponding to the HBM as previously shown [14]. The negative control BSA was injected (10 μl, 0.1 mg/ml in phosphate buffer) to confirm the complete coverage of the chip surface with lipid by the absence of non-specific binding. This HBM was then used as a model cell membrane surface to study the antimicrobial peptide-membrane binding.

2.2.3. Antimicrobial peptide binding to HBM system

Peptide solutions were prepared by dissolving magainin 1, melittin, and 21Q in phosphate buffer from 10 to 140 μM. The solutions (80 μl, 980 s) were injected over the lipid surface at a flow rate of 5 μl/min. The peptide solution was then replaced by phosphate buffer and the peptide-HBM complex allowed to dissociate for 1200 s. Since the peptides interact with the HBM through hydrophobic interactions, the regeneration of the HBM surface by removal of the bound peptide was not possible without also removing the phospholipid monolayer. The phospholipid monolayer was therefore completely removed with an injection of octyl glucoside and each peptide injection was performed on a freshly generated HBM surface. All binding experiments were carried out at 25°C. The affinity of the antimicrobial peptide-lipid monolayer binding event was determined from analysis of a series of response curves in each case, where the resultant sensorgrams were collected at ten different peptide concentrations injected over each lipid surface for each peptide. The peptide concentrations ranged from 50 μM to 140 μM for DMPC and from 10 μM to 100 μM for DMPG.

2.3. Circular dichroism (CD) measurements

CD measurements were carried out on a Jasco J-810 Circular Dichroism Spectropolarimeter (Jasco, Tokyo, Japan) between 190 and 250 nm using quartz cells of 0.1 cm path length at 25°C. The scan speed was 20 nm/min and the bandwidth 1.0 nm. The resolution was 0.1 nm with 1 s response. The cell temperature was stabilised using a peltier temperature controller. The CD instrument was calibrated with (+)-10-camphorsulphonic acid. The DMPC and DMPG liposomes were prepared as described above. The concentration of the lipid solutions was 2 mM. CD spectra of magainin 1, melittin and 21Q were measured in 0.02 M phosphate buffer (pH 6.8) and in the presence of DMPC or DMPG vesicles at a peptide concentration of 20 μM. Peptide concentrations were determined using an HP 845× UV-visible ChemStation spectrophotometer at 280 nm in phosphate buffer, and an extinction coefficient for melittin and 21Q of $\varepsilon_{280} = 5570\ m^{-1}\ cm^{-1}$ was used [15]. The

Table 1
Sequence and molecular weights of bioactive peptides

Peptide	Sequence	MW	Charge[a]
Melittin	H_2N-GIGAVLKVLTTGLPALISWIKRKRQQ-$CONH_2$	2847	6+
21Q	H_2N-GIGAVLKVLTTGLPALISWIQ-$CONH_2$	2150	2+
Magainin 1	H_2N-GIGKPLHSAGKPGKAPVGEIMKS-COOH	2410	4+

[a]Total net charge based on the number of positively and negatively charged amino acids.

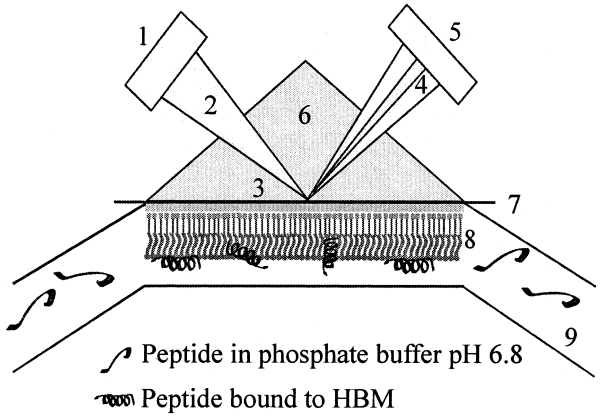

Fig. 1. The configuration of the SPR detector, sensor chip and flow channel in the BIAcore system. Real-time bimolecular interaction analysis (BIA) that uses SPR was used to monitor the interactions between the bioactive peptides and the membrane system. 1, light source; 2, polarised light; 3, opto interface; 4, reflected light; 5, detector array; 6, prism; 7, sensor chip HPA; 8, HBM; 9, flow cell.

concentration of magainin was determined by amino acid analysis. The peptide to lipid ratio was 1:100. In all measurements CD spectra of the same buffer and/or liposome solutions without peptides were applied as baseline. To obtain final CD spectra, the average of a series of five CD scans was accumulated for each sample. If required, spectra were smoothed using the Jasco Fast Fourier Transform algorithm. The helicity of each peptide was determined from the mean residue ellipticity at 222 nm ($[\theta]_{222}$, degcm^2/dmol) according to the relation $[\alpha] = 100 \times [\theta]_{222}/\theta_f$ and $\theta_f = -39\,500 \times (1 - 2.57/n)$ where $[\alpha]$ is the amount of helix, n is the residue number in the peptide and θ_f is the mean residue ellipticity of a helix of infinite residues [16].

2.4. Theoretical considerations

Fig. 1 shows the configuration of the SPR detector, sensor chip and flow channel in the BIAcore system. In the BIAcore X analytical system that uses SPR, the peptide (analyte, A) is in solution while the lipids (ligand, B) are immobilised on the biosensor surface forming a HBM system. In the present study the HBM system forms one wall of a microflow cell and the buffered solution of peptide is injected over the surface at a constant flow rate. As the peptide binds to the HBM, the instrument continuously monitors and measures the changes in the refractive index, given in resonance units (RU), at the surface of the HPA sensor chip to generate sensorgrams as shown in Fig. 2 [17–19]. During the binding process, the association (k_a) and dissociation (k_d) rate constants control the formation and breakdown of the complex (AB) at the sensor surface, as shown in Eq. 1.

$$A + B \underset{k_d}{\overset{k_a}{\Leftrightarrow}} AB \quad (1)$$

Using the resultant sensorgrams of each peptide, linearisation analysis using Excel 8.0 software (Microsoft, Redmond, WA, USA) and curve fitting with numerical integration using BIAevaluation 3.0 software (Biacore) were performed to derive estimates for kinetic constants including the association (k_a) and dissociation (k_d) rate constants.

2.4.1. Linearisation analysis

The sensorgrams resulting from the peptide-lipid interactions were analysed by linearisation analysis [18,19]. This method involves a simple linear trans-

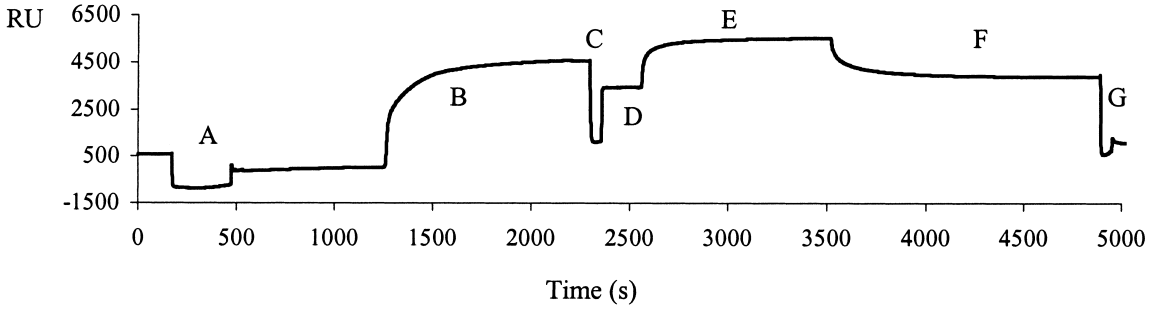

Fig. 2. Monitoring the lipid monolayer formation on the HPA sensor chip surface and peptide binding onto the HBM. A, cleaning the sensor chip surface by octyl glucoside; B, SUV deposition onto the HPA surface; C, removal of multilayers by NaOH; D, peptide injection over the HBM; E, adsorption of the peptide; F, dissociation of the peptide; G, regeneration of the surface.

formation of binding data to determine binding parameters. The limitation of this method is that it is only suitable for interpreting reactions that follow a simple bimolecular mechanism. The possible interpretation of the binding reaction that this analysis suggests, is that the peptide (P) simply binds to lipids (L) and/or inserts into the HBM with no other interactions involved as follows:

$$P + L \Leftrightarrow PL \quad (2)$$

The corresponding differential rate equation for this reaction model is:

$$dR/dt = k_a \times [C_P] \times R_{max} - (k_a \times [C_P] + k_d) \times R \quad (3)$$

where k_a and k_d are the association and dissociation rate constants respectively, R_{max} is the maximum signal which is proportional to the initial concentration of L, $[C_P]$ is the peptide concentration and R is the signal from the biosensor which is proportional to the amount of complex (PL).

To determine whether the peptide-lipid interactions can be described by a simple 1:1 bimolecular reaction, the association phase of the sensorgram of the particular peptide at all peptide concentrations was plotted against the response (dR/dt versus R). In the case of a simple bimolecular interaction the association rate (k_a) of each peptide can be easily determined from the slope of the dR/dt versus R curves against peptide concentration according to Eq. 3. The dissociation rate of each peptide can also be determined by linearising the dissociation phase of the highest concentration of the particular peptide by plotting $\ln(R_0/R)$ versus time (s). A linear slope should also be observed in the case of a simple bimolecular interaction and the slope can be used to calculate the dissociation rate (k_d) constant. R_0 is the response at the start of the dissociation phase and R is the response at time t. However, non-linear slopes reflect complex interactions and the rate constants cannot be accurately determined [19].

2.4.2. Numerical integration analysis

The sensorgrams for each peptide-lipid interaction were also analysed by curve fitting using numerical integration analysis [19,20]. The BIAevaluation software offers seven different reaction models to perform complete kinetic analyses of the peptide sensorgrams. Three different curve fitting algorithms were chosen for comparison, on the basis of what is known about the possible binding mechanisms of antimicrobial peptides. In order to distinguish between the possible binding models, the data were fitted globally by simultaneously fitting the peptide sensorgrams obtained at ten different concentrations. To improve the fit, the sensorgrams at each peptide concentration were fitted separately, i.e. non-globally.

First, each peptide-lipid system was analysed using the simple Langmuir binding, one-to-one reaction model. The binding mechanism described by this model is that the peptide (P) binds to lipids (L) and/or inserts into the HBM, as described in Section 2.4.1.

The two-state reaction model was also applied to each data set. This model describes two reaction steps which, in terms of peptide-lipid interaction, may correspond to:

$$P + L \Leftrightarrow PL \Leftrightarrow PL^* \quad (4)$$

where: (1) Peptide (P) binds to lipids (L) to give PL. (2) The complex PL changes to PL* which cannot dissociate directly to P+L and which may correspond to partial insertion of the peptide into the HBM. The corresponding differential rate equations for this reaction model are represented by:

$$dR_1/dt = k_{a1} \times C_A \times (R_{max} - R_1 - R_2) - k_{d1} \times R_1 - k_{a2} \times R_1 + k_{d2} \times R_2 \quad (5)$$

$$dR_2/dt = k_{a2} \times R_1 - k_{d2} \times R_2 \quad (6)$$

The parallel reactions model was also applied to each data set. This model assumes that two simple bimolecular interactions occur in parallel with different rate constants giving a complex bimolecular interaction as follows.

1. Peptide (P) binds to lipids (L).

$$P + L \Leftrightarrow P^*L \quad (7)$$

2. The bound peptide (P*) then provides a surface for the binding of additional peptide molecules, e.g. possible pore formation (T).

$$P^* + T \Leftrightarrow PT \quad (8)$$

The corresponding differential rate equations for this reaction model are:

$$dR_1/dt = k_{a1} \times C_p \times (R_{max} - R_1) - R_1 \times k_{d1} \quad (9)$$

$$dR_2/dt = k_{a2} \times C_{p^*} \times (R_{max} - R_2) - R_2 \times k_{d2} \quad (10)$$

3. Results

3.1. Biosensor study

In the present study the lipid binding properties of three bioactive peptides, magainin 1, melittin and the C-terminally truncated analogue of melittin (21Q), were investigated in the presence of zwitterionic or anionic lipid surfaces using real time, label free biosensor technology. To investigate the different membrane selectivity and binding affinity of these peptides, HBM systems composed of either zwitterionic (DMPC) or anionic (DMPG) lipids were used. Fig. 3 schematically shows the proposed stepwise formation of the supported lipid monolayer on the alkanethiol surface of the HPA sensor chip. The figure illustrates that the SUV adsorb spontaneously to form a supported lipid monolayer on the hydrophobic alkanethiol surface, providing a model cell membrane surface. Phosphate buffered solutions of each peptide were passed over the HBM surface at a constant flow rate. A typical sensorgram obtained for the pro-

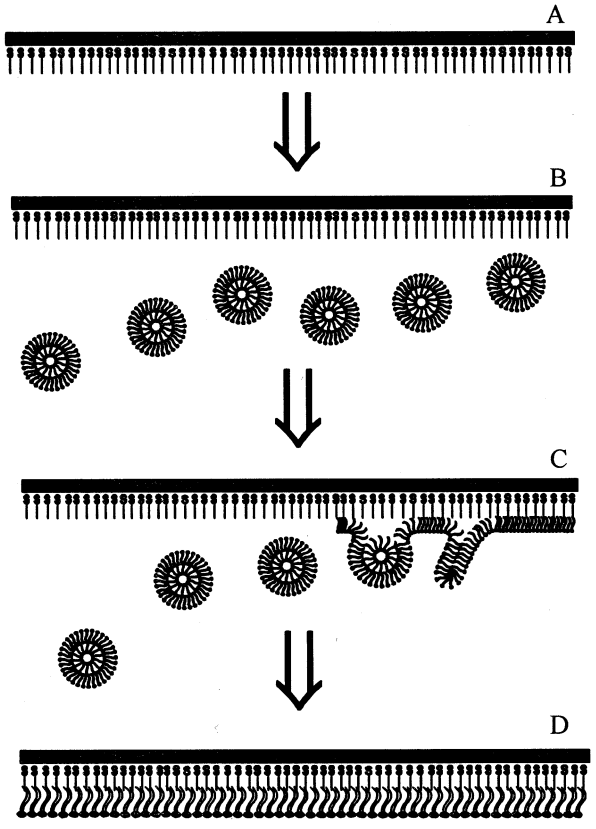

Fig. 3. Preparation of the HBM system. (A) The HPA chip is composed of long chain alkanethiol molecules covalently linked to the gold surface to form a flat hydrophobic alkanethiol surface. (B) SUV (50 nm) are applied to the sensor chip surface. (C) Liposomes adsorb to the surface spontaneously and (D) form a supported lipid monolayer.

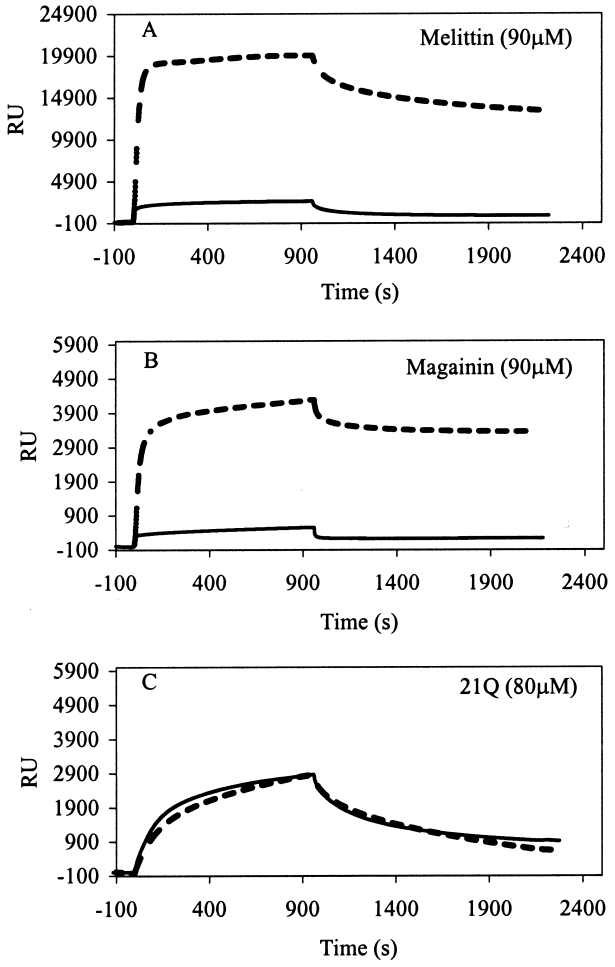

Fig. 4. Comparative peptide sensorgrams for (A) melittin (90 μM), (B) magainin 1 (90 μM) and (C) 21Q (80 μM) on DMPC (solid lines) and DMPG (dashed lines).

cess of lipid deposition, lipid monolayer formation on the HPA sensor chip and the binding of a peptide into the prepared lipid monolayer is shown in Fig. 2. The detected association rate of the peptides did not vary notably when the flow rate was varied from 1 to 10 μl/min, indicating that the interaction was not mass transport limited (data not shown).

Fig. 4 shows the comparative sensorgrams obtained for each peptide with both lipids. Initial inspection of the shape of each sensorgram reveals different binding kinetics with significant differences in both association and dissociation rates for both lipid surfaces. In particular, the sensorgrams indicate that the peptides bind to the lipid surfaces in a biphasic manner. The initial association of the peptide to the lipid surface starts as a very fast process, which then slows down considerably towards the end of the peptide injection and does not reach equilibrium. The dissociation of the HBM bound complex follows a similar pattern, with the signal falling rapidly at the end of injection since the peptide is no longer present and the buffer flow removes a large amount of free or weakly bound peptide, followed by a much slower step. Typically, the peptide sensorgrams did not return to zero, indicating that a proportion of the peptide remained bound to the surface or inserted into the HBM. This was observed for almost all peptide-lipid combinations with the exception of 21Q with DMPG.

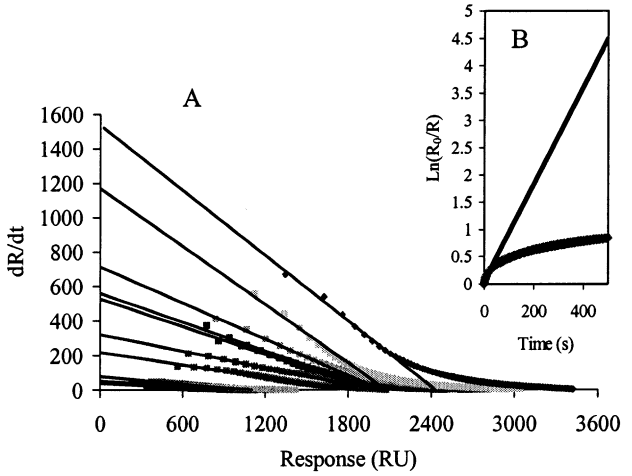

Fig. 5. Analysis by linearisation for the binding of melittin to DMPC. The linearisation of (A) association and (B) dissociation phase data resulted in curved plots, reflecting a complex bimolecular interaction for each peptide.

Different responses, measured in RU, were obtained with the differently charged lipid surfaces directly indicating that a higher proportion of magainin 1 and melittin bound to the anionic DMPG than to zwitterionic DMPC and that a higher proportion of melittin bound to both lipids than the truncated 21Q analogue. In addition, the shape of the sensorgrams also reflects that melittin bound more rapidly than 21Q to both lipids. In contrast, similarly shaped sensorgrams were obtained for 21Q on DMPC and DMPG, which indicates similar kinetics of 21Q for both lipids. Using the peptide sensorgrams, linearisation analysis and curve fitting with numerical integration were then performed to derive estimates for the association (k_a) and dissociation (k_d) rate constants and the binding affinity of the peptide-lipid interactions.

3.1.1. Linearisation

The linearisation method is widely used to estimate the rate constants for interactions that follow a simple bimolecular mechanism or Langmuir interaction (see Eq. 1) [18,19]. Using this method the possibility of a simple bimolecular interaction was eliminated by linearising the association phase data of the sensorgrams and the dissociation phase data of the highest concentration peptide sensorgram as described in Section 2.4. Fig. 5A,B show the linearisation of the association phase and dissociation phase data for the binding of melittin to DMPC. It is evident from this figure that curved plots were obtained at all peptide concentrations, and similar data were observed for melittin with DMPG and 21Q and magainin 1 on both DMPC and DMPG. Since the plots should appear linear for a simple bimolecular interaction, the results indicate that the peptide-lipid binding reactions are more complex than can be described by a simple 1:1 interaction. Alternative methods were then used to derive thermodynamic constants.

3.1.2. Numerical integration analysis

Numerical integration analysis that uses non-linear analysis to fit an integrated rate equation directly to the sensorgrams was employed. Fitting the peptide sensorgrams both globally and non-globally, a poor fit was obtained using the simplest 1:1 Langmuir binding model (data not shown), confirming that this model does not represent the lipid binding mech-

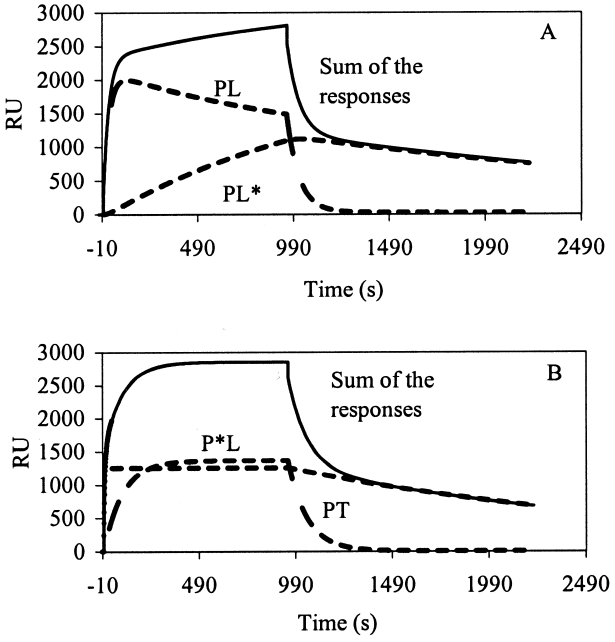

Fig. 6. Analysis by numerical integration for the binding of melittin to DMPC. Fitted sensorgrams obtained using (A) the two-state reaction system and (B) the parallel reactions system.

anism of antimicrobial peptides. However, significantly improved fit was obtained using numerical integration of the two-state reaction model and the parallel reactions model on the binding sensorgrams.

Fig. 6A,B show the fitted sensorgrams obtained using the two-state reaction system and the parallel reactions system, respectively. The figures also show the component signals associated with the two bound forms of the peptide PL and PL* or PT and P*L, which make up the output response. For the two-state reaction and the parallel reactions models, the first step is most likely to be the initial binding of the peptide to the membrane surface to give either PL or P*L. The second steps are then either insertion of the peptide into the membrane interior (PL*) and/or subsequent binding of additional peptide to initiate pore formation (PT). The relative rate constants for each of these states will determine which model is most appropriate for these peptide-membrane interactions.

Kinetic analysis of the interactions was carried out using these two models. A set of peptide sensorgrams with ten different analyte concentrations was used to estimate the kinetic parameters. The average values for the rate constants obtained from the analysis are listed in Table 2 and 3 along with the association constant values (K_A, K_{A1} and K_{A2}) for both systems. The association constants were calculated from the association and dissociation rate constants established by both reaction models for the differently surface charged HBM systems. The two-state reaction model supplies a single K_A value while the parallel reactions model provides two K_A values, K_{A1} and K_{A2}. It is possible that K_{A1} describes the initial binding of the peptide to the membrane, and K_{A2} relates to the subsequent peptide-peptide interaction. This phenomenon has also been recently observed for the binding of model amphipathic peptides to mixed liposomes containing phosphatidylcholine/phosphatidylglycerol/phosphatidylethanolamine [21]. The association constants determined by the two-state reaction model, listed in Table 2, demonstrated that magainin 1 and melittin had a much higher binding affinity for the anionic DMPG than for the zwitterionic DMPC. Melittin also displayed a much higher binding affinity for both lipids than magainin 1. This is consistent with previous studies, which showed that both peptides bind more strongly to negatively charged liposomes than zwitterionic liposomes [7,22–24]. In particular, the magnitudes of K_A values obtained are similar to those previously re-

Table 2
Association (k_{a1}, k_{a2}) and dissociation (k_{d1}, k_{d2}) rate constants determined by numerical integration using the two-state reaction model, and the affinity constant (K) determined as $(k_{a1}/k_{d1})\times(k_{a2}/k_{d2})$

Peptide	Lipid type	k_{a1} (1/Ms)	k_{d1} (1/s)	k_{a2} (1/Ms)	k_{d2} (1/s)	K (1/M)
Melittin	DMPC	209	134×10^{-4}	8.0×10^{-4}	3.8×10^{-4}	3.3×10^{4}
	DMPG	1 671	41×10^{-4}	3.5×10^{-4}	0.7×10^{-4}	206×10^{4}
21Q	DMPC	51	62×10^{-4}	9.7×10^{-4}	3.5×10^{-4}	2.3×10^{4}
	DMPG	23	59×10^{-4}	18×10^{-4}	7.6×10^{-4}	0.9×10^{4}
Magainin 1	DMPC	86	565×10^{-4}	8.0×10^{-4}	1.3×10^{-4}	0.9×10^{4}
	DMPG	333	58×10^{-4}	11.7×10^{-4}	0.7×10^{-4}	91×10^{4}

Table 3
Association (k_{a1}, k_{a2}) and dissociation (k_{d1}, k_{d2}) rate constants determined by numerical integration using the parallel reactions model, and the affinity (K_{A1}, K_{A2}) constants determined as k_{a1}/k_{d1} and k_{a2}/k_{d2}, respectively. k_{a1}, k_{d1} and K_{A1} are associated with the peptide-lipid interaction, while k_{a2}, k_{d2} and K_{A2} values are associated with the putative peptide-peptide interaction

Peptide	Lipid type	k_{a1} (1/Ms)	k_{d1} (1/s)	k_{a2} (1/Ms)	k_{d2} (1/s)	K_{A1} (1/M)	K_{A2} (1/M)
Melittin	DMPC	74	4.1×10^{-4}	1 001	125×10^{-4}	18×10^{4}	11×10^{4}
	DMPG	3 079	3.7×10^{-4}	13 129	97×10^{-4}	838×10^{4}	135×10^{4}
21Q	DMPC	26	2.5×10^{-4}	171	76×10^{-4}	10×10^{4}	2.3×10^{4}
	DMPG	12	13×10^{-4}	67	81×10^{-4}	0.9×10^{4}	0.8×10^{4}
Magainin 1	DMPC	20	2.6×10^{-4}	919	681×10^{-4}	8.5×10^{4}	1.4×10^{4}
	DMPG	687	1.8×10^{-4}	2 251	206×10^{-4}	380×10^{4}	11×10^{4}

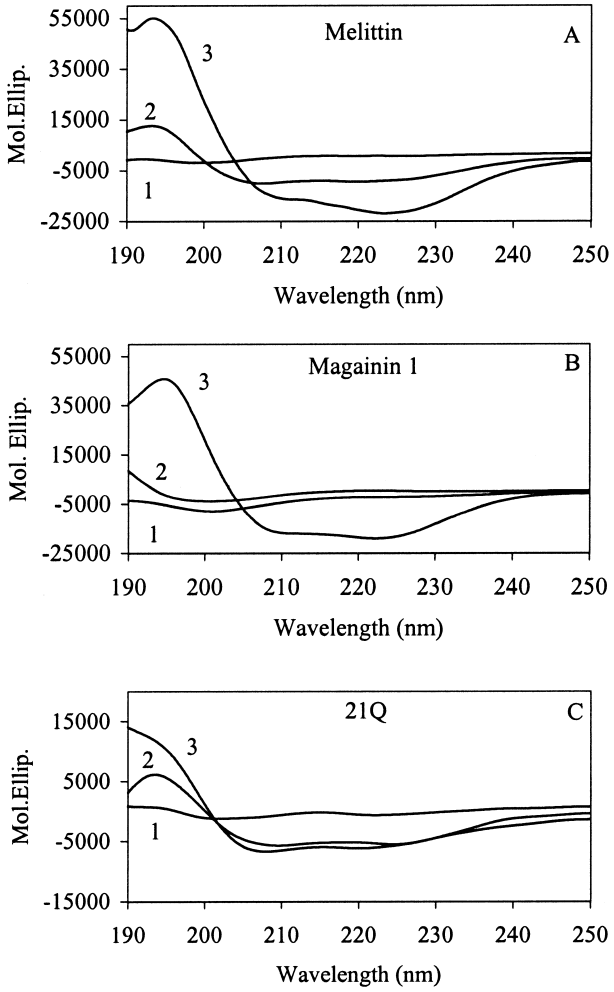

Fig. 7. CD spectra of (A) melittin, (B) magainin 1 and (C) 21Q in 20 mM phosphate buffer pH 6.8 (1) and in the presence of DMPC (2) or DMPG (3) liposomes. The peptide concentration is 20 μM, the peptide:lipid ratio is 1:100.

ported for melittin and magainin [25–27]. The truncated melittin analogue, 21Q, exhibited lower binding affinity than melittin for both lipids. In addition, 21Q had almost similar binding affinity for the zwitterionic and negatively charged phospholipid surfaces. Analysis of the sensorgrams using the parallel reactions model yielded similar results (Table 3) to the two-state reaction model in terms of the relative binding affinity of each peptide for both lipids.

3.2. Circular dichroism study

CD measurements were also performed to analyse the conformation of the peptides in phosphate buffer and in the presence of differently surface charged liposomes. Fig. 7 shows the CD spectra obtained for magainin 1, melittin and the truncated analogue of melittin (21Q) in phosphate buffer and in DMPC and DMPG liposome solutions. The % helix values were determined from $[\theta]_{222}$ [16] and are listed in Table 4. None of the peptides showed any secondary structure in phosphate buffer nor did magainin 1 in the presence of zwitterionic DMPC liposomes. In contrast, melittin and its analogue, 21Q, adopted α-helical conformation in the presence of DMPC

Table 4
% α-helicity of peptides in phosphate buffer (pH 6.8) and in the presence of DMPC and DMPG liposomes at 25°C

	% α-helix[a]		
	Melittin	21Q	Magainin 1
Buffer	0	0	0
DMPC	26	18	0
DMPG	58	18	57

[a]% α-helicity determined according to [15].

liposomes and the helical content was calculated to be 26% and 18%, respectively. All of the peptides adopted α-helical conformation in anionic DMPG liposome solution with a helical content of 57%, 58% and 18% found for magainin 1, melittin and 21Q, respectively.

4. Discussion

SPR analysis is now widely used to study antibody-antigen, protein-protein, DNA-protein, DNA-DNA, receptor-ligand interactions [17,28–32]. More recently, SPR has also been applied to the study of biomembrane-based systems [14,33–37]. The present study was undertaken with the aim of applying SPR analysis to study the direct binding of peptides to phospholipid membranes and to derive information regarding the membrane selectivity and structure-function relationship of antimicrobial peptides through the binding affinity data. Since very few studies have been conducted in which SPR has been used to examine peptide-membrane interactions [38], no complete kinetic analysis or experimental design has been investigated for such interactions.

The antimicrobial peptides magainin 1, melittin and a C-terminally truncated analogue of melittin (21Q) were used in this study. Magainin 1 is a 23 amino acid long amphipathic peptide that has been isolated from the skin of the African clawed frog *Xenopus laevis*. It possesses high antimicrobial, fungicidal and virucidal activity and kills bacteria by permeabilising its cell membrane [1,7]. Melittin is a 26 amino acid long amphipathic peptide that has been isolated from the European honey bee (*Apis mellifera*) venom. It has a moderate antibacterial and antifungal activity and is highly haemolytic [3,39]. The C-terminally truncated melittin analogue, 21Q, has the same sequence as melittin but residues 21–25 are omitted from the C-terminus. 21Q possesses lower antibacterial and haemolytic activity than melittin [40]. Different hypotheses have been proposed to explain the cytolytic activity of these peptides. Fig. 8 shows two different models of pore formation for melittin and magainin. Both peptides are unstructured in aqueous solutions and form an amphipathic α-helical conformation upon contact with lipids. In the case of melittin, the evidence suggests that the peptide inserts into the hydrocarbon region of the target cell membrane and forms transmembrane pores by the assembly of several monomers via a barrel-stave mechanism. The exterior of the formed peptide ring contacts with the hydrocarbon region of the bilayer [5,41–43]. In the case of magainin, the peptides align parallel to the outer membrane surface disturbing the membrane structure. At high peptide concentration, the peptide inserts into the membrane and creates a toroidal pore. During the whole process, the peptides remain in contact with the head group region of the lipid bilayer. Upon disintegration of the toroidal pore, peptides can translocate into the inner leaflet of the membrane [42,44–46]. Although different pore formation processes are proposed in these models, the formation of an amphipathic helical structure is a common feature for both peptides during the interaction with membrane surfaces. However, information on the physicochemical properties of antimicrobial peptides, which give rise to the differential binding of various peptides to different lipids, is not yet well understood. In the present study differently surface charged HBM systems were used to investigate the interactive properties of antimicrobial peptides during the initial binding and partial insertion into a membrane.

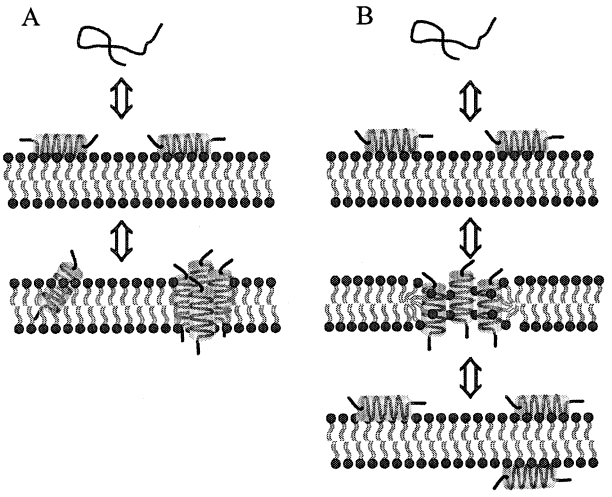

Fig. 8. Schematic representation of the mechanism of pore formation for (A) melittin and (B) magainin. See text for details.

To perform the membrane binding study, the HBM system was prepared by adsorption of small unilamellar vesicles onto the surface of an HPA sensor chip that resembles the surface of a cellular mem-

brane. Buffered solution of each peptide was then applied over the lipid surface and the resultant sensorgrams were analysed by linearisation and numerical integration to perform kinetic analysis. The results of the present study demonstrated that the antimicrobial peptide-lipid interaction possesses complicated kinetics, which reflects a complex multistate binding mechanism. The linearisation analysis and the numerical integration analysis using the Langmuir binding model (data not shown) indicated that this model is not applicable to the analysis of the complex peptide-lipid interactions since it is based on a simple bimolecular mechanism. However, both the two-state reaction and parallel reactions model gave significantly improved fit to the data, suggesting that there are likely to be at least two steps involved in the interaction between the peptide and HBM system. In the case of the two-state reaction model, the peptides may first bind to the lipid head groups and then insert further into the hydrocarbon region of the membrane. However, the peptide may not be able to fully insert into the hybrid bilayer due to the covalent attachment of the alkanethiol chains to the gold surface. The parallel reactions model assumes two simple bimolecular interactions running parallel with different rate constants giving a complex bimolecular interaction. One possible molecular mechanism may involve a peptide-lipid interaction when the peptides initially bind to the HBM and then partially insert into the hybrid bilayer which may lead to limited disruption of the adsorbed phospholipid layer. The other possible molecular mechanism may involve a peptide-peptide interaction when the peptides bind to the already bound peptides. While it is possible that the interactions between antimicrobial peptides and membranes are even more complex than can be described by these two models, they provide a more appropriate kinetic analysis of the interactions than the 1:1 binding model.

The biosensor binding data were also correlated with the conformation of each peptide in the presence of either zwitterionic DMPC or anionic DMPG liposomes determined by CD. The biosensor data showed that melittin bound more strongly to zwitterionic DMPC than magainin 1, and CD showed that melittin adopted α-helical conformation in the presence of DMPC liposomes but magainin 1 had no secondary structure. The biosensor data also showed that both melittin and magainin 1 exhibited much higher binding affinity for the anionic DMPG than for DMPC and CD indicated that the helical content of both peptides was considerably higher in the presence of DMPG liposomes. This higher helical content directly correlated with higher lipid binding affinity, which demonstrates that the formation of an α-helical structure is an important requirement in the binding process, presumably due to the amphipathic nature of each peptide helix.

The role of the C-terminal positive residues of melittin was also studied using the C-terminally truncated analogue (21Q) of melittin. The biosensor and CD results clearly demonstrated that the differences in the structure of melittin and 21Q influenced their lipid binding properties. 21Q had a considerably slower initial association with both lipids than melittin. CD showed that both peptides adopted α-helical conformation in the presence of zwitterionic DMPC and anionic DMPG liposomes but the helical content of 21Q remained at a similar lower level in both lipid environments. Overall, melittin adopted a considerably higher degree of helical structure in the presence of DMPG and bound stronger to both lipids than 21Q, showing that the positively charged C-terminal residues of melittin contribute significantly to the binding affinity of melittin for DMPG. Thus, the absence of positively charged C-terminal residues in 21Q resulted in a loss of binding specificity with similar low binding affinities observed for this peptide with DMPC and DMPG. Comparison of the results of melittin and 21Q thus indicates that the positive tail of melittin allows it to bind more rapidly and more strongly to the anionic lipids by electrostatic interactions, thereby enhancing the subsequent hydrophobic binding. These results also clearly demonstrate the role of electrostatic interactions in the initial orientation and binding of these peptides to membrane. In particular, these results suggest that electrostatic interactions may correspond to the initial rapid phase since 21Q exhibited a slower association phase than melittin. The subsequent insertion/peptide aggregation step may then correspond to the slower second phase of binding.

The biosensor and CD results presented here can also be correlated with the biological activity and binding properties of these peptides observed in pre-

vious studies. For example, it has been shown that magainin has a low haemolytic activity with biomembranes containing zwitterionic DMPC in the outer leaflet of the cellular membrane [47]. Other studies have also suggested that the membrane selectivity and the cytolytic and antimicrobial activity of magainin are related to the hydrophobicity of magainin which is too low to effectively associate with membranes which are mainly composed of zwitterionic phospholipids [7,22,48]. The present study also demonstrated a weak affinity of magainin 1 for zwitterionic DMPC, which predominates in eucaryotic membranes, and which may be partly responsible for its low haemolytic activity. The very strong binding of magainin 1 to the negatively charged lipids and the high helical content in anionic DMPG liposome solution agree with the fact that magainin preferentially acts on bacterial cells containing large amounts of anionic phospholipids via electrostatic interactions [1,22].

The experimental data presented here also showed that melittin interacts strongly with both zwitterionic and anionic lipids, which correlates with the fact that melittin binds and lyses both bacterial and eucaryotic cells [7,22]. Previous studies also found that melittin is 5 times more haemolytic than its C-terminally truncated analogue, 21Q [40]. Schroeder and coworkers also showed that the C-terminal charges of melittin are vital for haemolytic activity, since the deletion of the charged residues (KRKRQQ) from the C-terminus of melittin resulted in the loss of haemolytic activity [6]. The low haemolytic activity of the C-terminally truncated melittin analogue [6,40] thus suggests that the positive charges are important for membrane recognition providing the initial electrostatic binding. The biosensor results in this study also suggest that the positive charges actually increase the lipid binding affinity of melittin, thereby enhancing its haemolytic activity.

5. Conclusions

We found that biosensor technology represents a new and useful experimental procedure to rapidly determine the relative affinity of bioactive peptides for phospholipid surfaces. In particular, this technique can provide information on the role of electrostatic interactions in membrane binding and provide an insight into the structure-biological activity relationship. The results demonstrated that differences in antimicrobial peptide-lipid membrane affinity and in the kinetics of lipid binding of these peptides can be easily determined, which correlate with their experimentally observed rate of haemolytic activity, antimicrobial activity and membrane selectivity.

Acknowledgements

The financial support of the Australian Research Council is gratefully acknowledged.

References

[1] M. Zasloff, Proc. Natl. Acad. Sci. USA 84 (1987) 5449–5453.
[2] M.S.P. Sansom, Prog. Biophys. Mol. Biol. 55 (1991) 139–235.
[3] E. Habermann, Science 177 (1972) 314–322.
[4] H. Steiner, D. Hultmark, Å. Engström, H. Bennich, G.H. Boman, Nature 292 (1981) 246–248.
[5] M. Dathe, T. Wieprecht, Biochim. Biophys. Acta 1462 (1999) 71–87.
[6] G. Saberwal, R. Nagaraj, Biochim. Biophys. Acta 1197 (1994) 109–131.
[7] K. Matsuzaki, K. Sugishita, N. Fujii, K. Miyajima, Biochemistry 34 (1995) 3423–3429.
[8] S.E. Blondelle, K. Lohner, M.-I. Aguilar, Biochim. Biophys. Acta 1462 (1999) 89–108.
[9] W.C. Wimley, S.H. White, Anal. Biochem. 213 (1993) 213–217.
[10] R.E. Jacobs, S.H. White, Biochemistry 28 (1989) 3421–3437.
[11] J.B. Heymann, S.D. Zakharov, Y.L. Yang, W.A. Cramer, Biochemistry 35 (1996) 2717–2725.
[12] J.M. Delfino, S.L. Schreiber, F.M. Richards, J. Am. Chem. Soc. 115 (1993) 3458–3474.
[13] D.E. Rivett, A. Kirkpatrick, D.R. Hewish, W. Reilly, J.A. Werkmeister, Biochem. J. 316 (1996) 525.
[14] M.A. Cooper, A.C. Try, J. Carroll, D.J. Ellar, D.H. Williams, Biochim. Biophys. Acta 1373 (1998) 101–111.
[15] E. Pérez-Payá, R.A. Houghten, S.E. Blondelle, J. Biol. Chem. 270 (1995) 1048–1056.
[16] Y.-H. Chen, J.T. Yang, K.H. Chau, Biochemistry 13 (1974) 3350–3359.
[17] S. Kumar, K. Gunnarsson, in: A.L. Harvey (Ed.), Advances in Drug Discovery Techniques, John Wiley and Sons, New York, 1998, pp. 97–114.
[18] T.A. Morton, D.G. Miszka, Methods Enzymol. 295 (1998) 268–294.

[19] T.A. Morton, D.G. Miszka, I.M. Chaiken, Anal. Biochem. 227 (1995) 176–185.
[20] R. Karlsson, A. Fält, J. Immunol. Methods 200 (1997) 121–133.
[21] N. Uematsu, K. Matsuzaki, Biophys. J. 79 (2000) 2075–2083.
[22] K. Matsuzaki, Biochim. Biophys. Acta 1462 (1999) 1–10.
[23] R.E. Hancock, T. Falla, M. Brown, Adv. Microb. Physiol. 37 (1995) 135–175.
[24] A.K. Ghosh, R. Rukmini, A. Chattopadhyay, Biochemistry 36 (1997) 14291–14305.
[25] G. Beschiaschvili, J. Seeling, Biochemistry 29 (1990) 52–58.
[26] M.R. Wenk, J. Seeling, Biochemistry 37 (1998) 3909–3916.
[27] S.A. David, V.I. Mathan, P. Balaram, Biochim. Biophys. Acta 1123 (1992) 269–274.
[28] A. Szabo, L. Stolz, R. Granzow, Curr. Opin. Struct. Biol. 5 (1995) 699–705.
[29] R.J. Fisher, M. Fivash, Curr. Opin. Biotechnol. 5 (1994) 389–395.
[30] B. Cheskis, L.P. Freedman, Biochemistry 35 (1996) 3309–3318.
[31] P. Nilsson, B. Persson, M. Uhlén, P.-Å. Nygren, Anal. Biochem. 224 (1995) 400–408.
[32] R. Karlsson, Anal. Biochem. 221 (1994) 142–151.
[33] M.A. Cooper, D.H. Williams, Anal. Biochem. 276 (1999) 36–47.
[34] E. Saenko, A. Sarafanov, N. Greco, M. Shima, K. Loster, H. Schwinn, D. Josic, J. Chromatogr. A 852 (1999) 59–71.
[35] G.M. Kuziemko, M. Stroh, R.C. Stevens, Biochemistry 35 (1996) 6375–6384.
[36] O.V. Rajaram, W.H. Sawyer, Biochem. Mol. Biol. Int. 39 (1996) 31–39.
[37] S. Terrettaz, T. Stora, C. Duschl, H. Vogel, Langmuir 9 (1993) 1361–1369.
[38] W. Wang, D.K. Smith, K. Moulding, H.M. Chen, J. Biol. Chem. 273 (1998) 27438–27448.
[39] M. Dathe, M. Schümann, T. Wieprecht, A. Winkler, M. Beyermann, E. Krause, K. Matsuzaki, O. Murase, M. Bienert, Biochemistry 35 (1996) 12612–12622.
[40] T.-H. Lee, D. Rivett, J. Werkmeister, D. Hewish, M.-I. Aguilar, Lett. Pept. Sci. 6 (1999) 371–380.
[41] Y. Shai, Biochim. Biophys. Acta 1462 (1999) 55–70.
[42] B. Bechinger, J. Membr. Biol. 156 (1997) 197–211.
[43] H. Vogel, F. Jähning, Biophys. J. 50 (1986) 573–582.
[44] B. Bechinger, Biochim. Biophys. Acta 1462 (1999) 157–183.
[45] K. Matsuzaki, Biochim. Biophys. Acta 1376 (1998) 391–400.
[46] S.J. Ludtke, K. He, W.T. Heller, T.A. Harroun, L. Yang, H.W. Huang, Biochemistry 35 (1996) 13723–13728.
[47] Z. Oren, Y. Shai, Biopolym. Pept. Sci. Sect. 47 (1998) 451–463.
[48] K. Matsuzaki, M. Fukui, N. Fujii, K. Miyajima, Biochim. Biophys. Acta 1070 (1991) 259–264.